



Analysis of a Vertical Pump in MADYN 2000

Nonlinear analyses can be carried out in MADYN 2000 since version 3.1, when nonlinear fluid film bearings were implemented for analyses with constant speeds. Since then nonlinear analyses with variable speed and new nonlinear objects were introduced: Nonlinear couplings, general nonlinear objects and in version 4.3 nonlinear rolling element bearings. Moreover, the robustness and analysis speed were continuously enhanced. In this newsletter the analysis of a vertical pump with water lubricated cylindrical fluid bearings and a rolling element bearing is described. It is also explained, why such a system requires nonlinear analyses.

Table of contents

1. General Background of Nonlinear Analyses for a Vertical Pump	1
2. Description of the System.....	2
3. Linear Analysis, Campbell Diagram	3
4. Nonlinear Analysis of a Run Up	5
5. Conclusions	7

1. General Background of Nonlinear Analyses for a Vertical Pump

In the present document a vertical pump with water lubricated bearings is analysed. Fluid film bearings are normally linearized around their static load, which yield the linear stiffness and damping coefficients. The linearized behaviour can give good results in a wide range of dynamic loads, which are in the best case small compared to the static load or at least do not exceed it. If the static load is zero or small, then strictly speaking the behaviour is always nonlinear. Moreover, in the present example the rotor is unstable, because it has unloaded cylindrical bearings. A linear analysis does not tell at which level the unstable system stabilizes (limit cycle). To get this result, which is essential for an assessment of the rotor behaviour, a nonlinear analysis is necessary.

Although in cases such as our vertical pump the behaviour can only be correctly simulated with nonlinear analyses, they are rarely carried out in practical engineering for the following reasons: In many cases linear analyses are sufficient to get correct answers for the design of a machine although real machines are always nonlinear to some extent. Nonlinear analyses take considerably more effort than well-established linear analyses such as undamped critical speed maps, damped Campbell diagrams and damped unbalance response analyses. Most of these linear analyses are required by standards such as API standards, whereas so far, no standard asks for nonlinear analyses. Nonlinear analyses normally take a much bigger effort for the following reasons: The nonlinear effects must be modelled, analysis times are much longer (usually the nonlinear equations are integrated in the time domain by solvers such as Runge Kutta), the solver may be numerically unstable, and the resulting behaviour can be complex requiring some effort for the interpretation of the result.

To avoid nonlinear analyses even in systems as presented here, the dynamic force is sometimes taken as static force to linearize the bearings, which of course is physically completely wrong and cannot provide correct results in general.

The proven, robust standard rotordynamic tool MADYN 2000 facilitates correct nonlinear analyses allowing to correctly simulate the behaviour of rotors such as a vertical pump. Linear analyses can be quite meaningless for such machines apart from allowing to check the stability.

The present example has a practical background, although a rotor in this form does not exist. It is derived from a real application.



2. Description of the System

The model of the vertical pump is shown in figure 2.1. The upper part with a motor is on the left side. The pump has only one impeller at the bottom shown on the right side. The pump rotor is shaded in blue. The casing of the pump, which is a pipe, is modelled as a shaft with zero speed. It is shaded in grey (partly visible as a black line). The pipe is fixed to a foundation, which is denoted as customer support in the model. It consists of a flange of the pipe. The flange is fixed with a general spring to the ground, which represents the stiffness of the foundation and introduces anisotropy to the system. The motor rotor is not modelled as part of the shaft, since it is coupled to the pump shaft with a flexible coupling. The whole motor including its housing is modelled as a rigid mass fixed to the flange at the customer support stiffness (the sphere in figure 2.1). The distance of the centre of gravity to the support is bridged with a rigid element.

The pump shaft is supported in the pipe with an angular contact rolling element bearing, which also carries the axial load of 5000N. The upper bush and casing bearing are closed cylindrical bearings. The other bush bearings are cylindrical bearings with 3 equal pads and a deep groove between the pads. The ambient pressure of the upper bush bearing corresponds to the pump discharge pressure of 10bar. For the other bush bearings and the casing bearing the Archimedes hydrostatic pressure adds to the discharge pressure, which is about 1bar for the lowest bearing. The elevated ambient pressure influences the cavitation, which is considered in the bearing model with a 2-phase model. A contact stiffness to account for a surface roughness of 10 μ m has been considered for all bearings.

Only lateral degrees of freedom (displacement in the radial 2,3 direction and rotation about these axes) are considered in the current model although the angular contact ball bearing couples the lateral degrees of freedom with the axial direction. The axial direction of the rolling element bearing stiffness matrix is reduced by a Guyan reduction, which implies that the rotor is free in axial direction (no other constraint apart from the ball bearing).

The mass of the enclosed water is added to the pipe mass. For the rotor an added mass according to the formula in equation 1.1¹ has been used to estimate the effect. It yields a mass of about 3% of the rotor mass and therefore is neglected.

$$\mu = \pi \delta \frac{\rho D^3}{8s} \quad (1.1)$$

with μ as the added mass per length, δ as the density, OD as the rotor outer diameter and s as the radial clearance between rotor and pipe, which is very large for our case (≈ 2 OD).

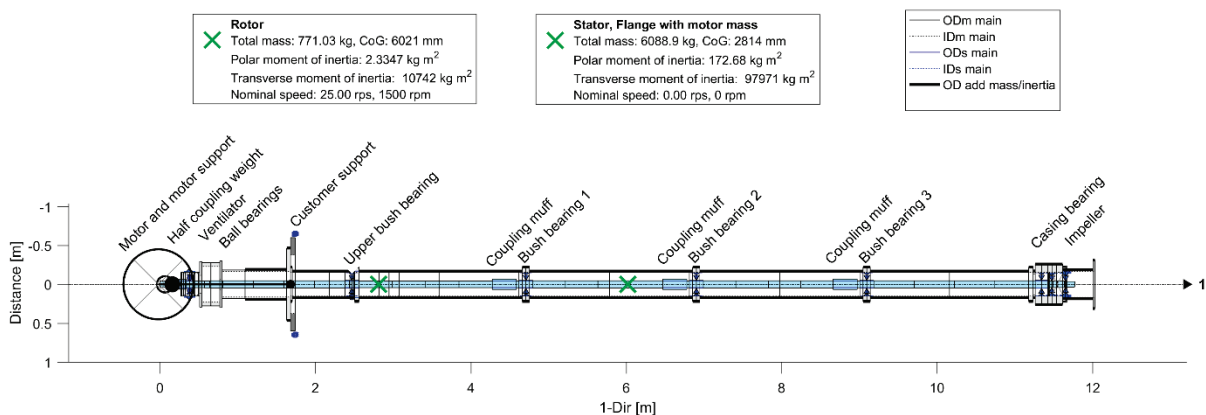


Fig. 2.1: Model of the vertical pump

¹ Amoser, M.: Strömungsfelder und Radialkräfte in Labyrinthdichtungen hydraulischer Strömungsmaschinen. Dissertation ETH Zürich Nr.11150 (1995)



3. Linear Analysis, Campbell Diagram

The linear analyses are carried out with the bearing stiffness and damping coefficients resulting from a linearization with no load for the fluid bearings and the axial load for the rolling element bearing. The rolling element bearing has no damping.

The Campbell diagram for a speed range up to 150% speed and a frequency range to 50Hz, which corresponds to two times nominal speed can be seen in figure 3.1. The corresponding mode shapes can be seen in figure 3.2. Note, that the colours for corresponding modes are the same in both figures. The dashed line in the shape plot represents the pipe deformation and the solid line the rotor deformation. The shapes are shown in two projections at the instant when the maximum deflection occurs. The two planes for the projections are indicated in the plot next to the shape. The first projection with the fat line is into the plane defined by the maximum deflection and the rotor axis, the second projection with the thin line is into the perpendicular plane. The mean global orbit shape² according to the value between ± 1 calculated for the whirling direction and direction of whirling are indicated as well.

The first two modes are a cantilever like bending of the pipe and the rotor in two perpendicular directions. There is almost no relative displacement between rotor and pipe. The next modes are bending modes of the rotor with increasing order and increasing relative displacement. The modes appear as elliptically forward and backward whirling modes. They are elliptic due to the anisotropy of the support stiffness. The forward modes with relative displacement in the bearings become unstable (mode 4, 5, 7, 9) if their frequency is below 50% speed, which is the whirling speed of the fluid in the cylindrical bearings.

Parameter Variation Analysis

Type: Campbell Diagram
 Analysis: 11-Jul-2017 14:42 - 18 rel.speeds (0.15...1.5), bearing loads from SAN

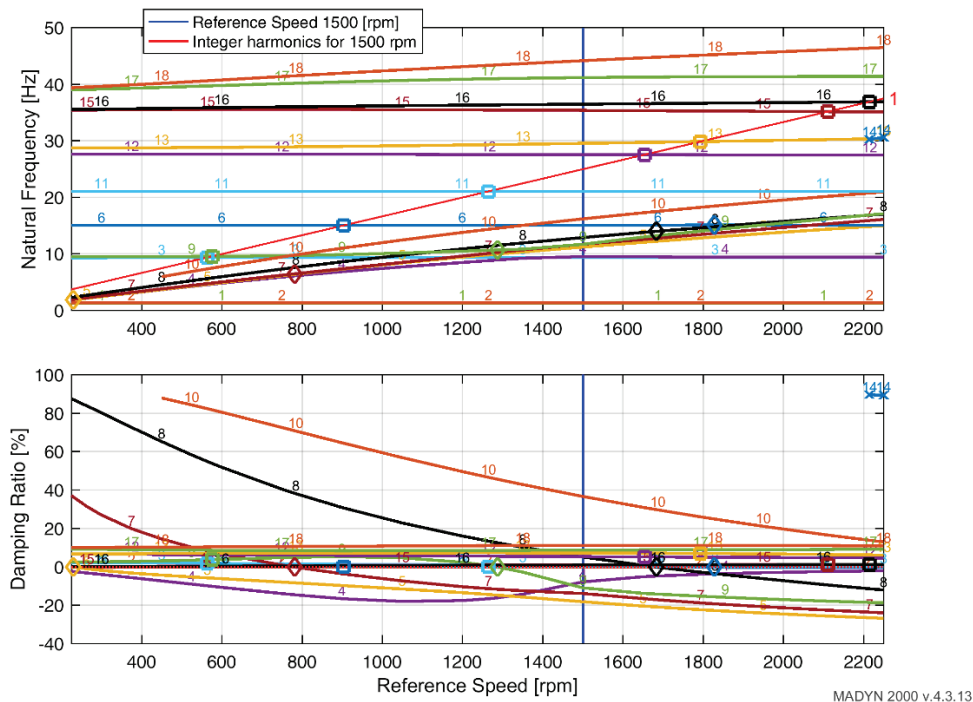


Fig. 3.1: Campbell diagram

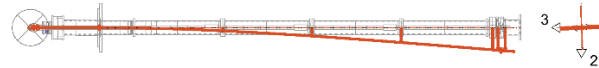
² New in version 4.4.



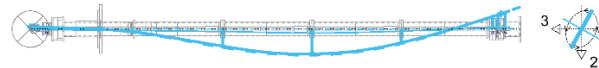
Shape for: 1500.00 rpm
 Mode: 1
 Frequency: 1.34 Hz
 80.2 cpm
 Damping Ratio: -0.0 %
 Whirling direction: -0.02



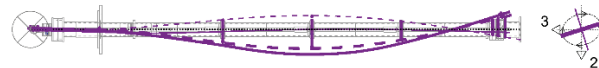
Shape for: 1500.00 rpm
 Mode: 2
 Frequency: 1.35 Hz
 81.3 cpm
 Damping Ratio: -0.0 %
 Whirling direction: +0.02



Shape for: 1500.00 rpm
 Mode: 3
 Frequency: 9.41 Hz
 564.5 cpm
 Damping Ratio: 0.9 %
 Whirling direction: -0.72



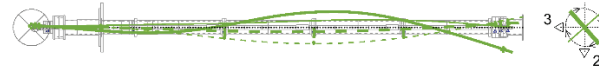
Shape for: 1500.00 rpm
 Mode: 4
 Frequency: 9.57 Hz
 574.0 cpm
 Damping Ratio: -7.7 %
 Whirling direction: +0.78



Shape for: 1500.00 rpm
 Mode: 5
 Frequency: 11.24 Hz
 674.7 cpm
 Damping Ratio: -18.0 %
 Whirling direction: +0.99



Shape for: 1500.00 rpm
 Mode: 9
 Frequency: 11.73 Hz
 703.6 cpm
 Damping Ratio: -10.8 %
 Whirling direction: +0.91



Shape for: 1500.00 rpm
 Mode: 7
 Frequency: 11.75 Hz
 704.8 cpm
 Damping Ratio: -13.8 %
 Whirling direction: +0.96



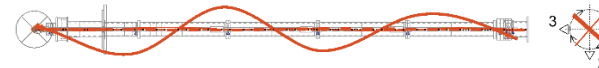
Shape for: 1500.00 rpm
 Mode: 8
 Frequency: 12.92 Hz
 775.4 cpm
 Damping Ratio: 5.3 %
 Whirling direction: +0.98



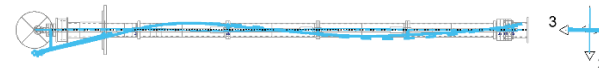
Shape for: 1500.00 rpm
 Mode: 6
 Frequency: 15.08 Hz
 904.9 cpm
 Damping Ratio: 0.2 %
 Whirling direction: +0.06



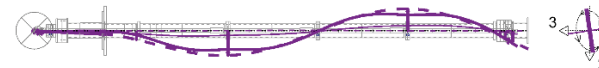
Shape for: 1500.00 rpm
 Mode: 10
 Frequency: 16.22 Hz
 973.5 cpm
 Damping Ratio: 36.8 %
 Whirling direction: +0.99



Shape for: 1500.00 rpm
 Mode: 11
 Frequency: 21.08 Hz
 1264.9 cpm
 Damping Ratio: 0.2 %
 Whirling direction: -0.04



Shape for: 1500.00 rpm
 Mode: 12
 Frequency: 27.58 Hz
 1654.6 cpm
 Damping Ratio: 5.4 %
 Whirling direction: -0.67



Shape for: 1500.00 rpm
 Mode: 13
 Frequency: 29.58 Hz
 1774.5 cpm
 Damping Ratio: 7.3 %
 Whirling direction: +0.45



Fig. 3.2: Natural modes at 1500rpm



4. Nonlinear Analysis of a Run Up

Since the linear system is unstable, a nonlinear analysis must be carried out to determine limit cycles revealing a realistic vibration level of the rotor. A nonlinear run up analysis with an unbalance of G10 at the impeller as shown in figure 4.1 has been carried out. The reference mass for the G value is the rotor section at the impeller. The run up has been carried out until 150% speed, although the rotor only runs at 100% speed. The run up time is 10s.

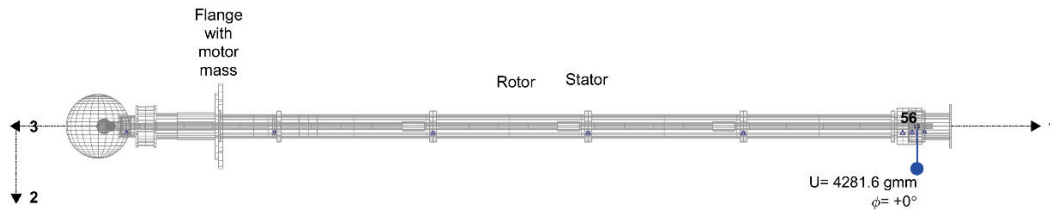


Fig. 4.1: Unbalance load for the run up

Results of this analysis can be seen in the following figures: The absolute displacements of the pipe at the bearing locations in figure 4.2, the orbits of the relative displacements in the fluid bearings at different speeds in 4.3 and the 3D shape at about 1500rpm in figure 4.4.

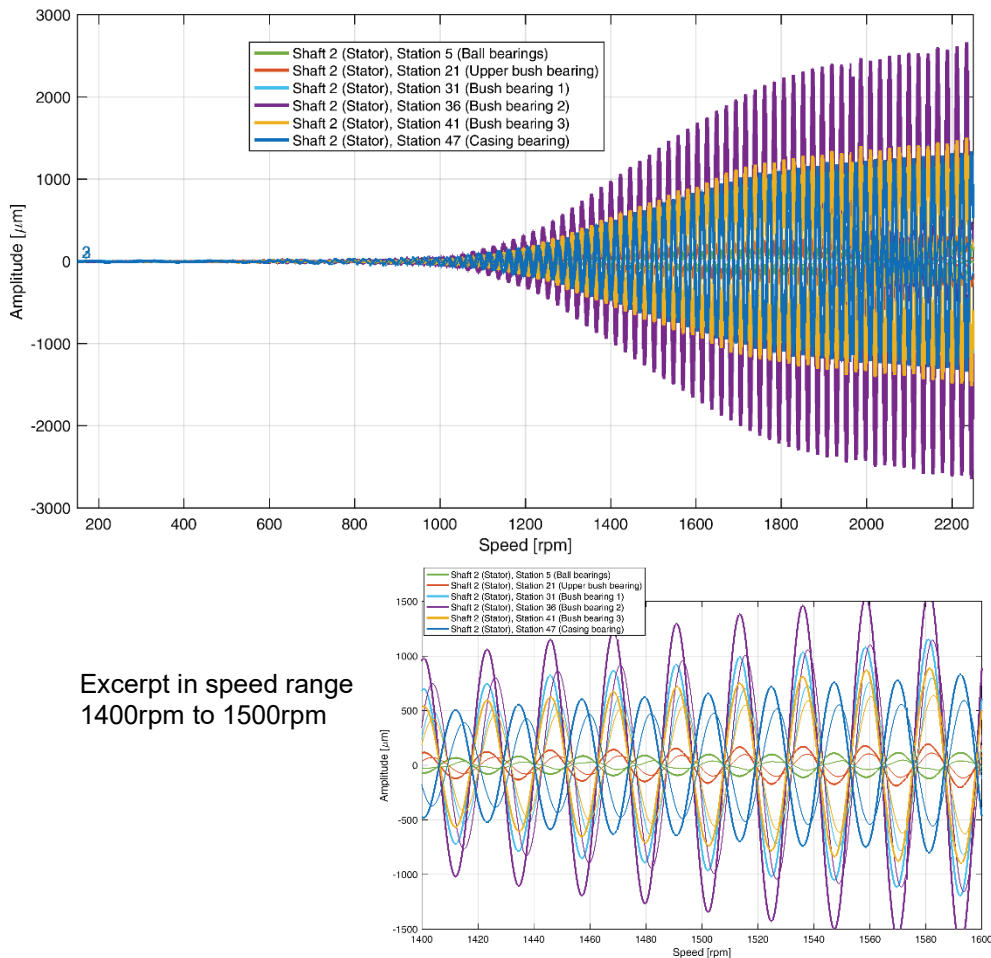


Fig. 4.2: Absolute vibration of the pipe at the bearing locations

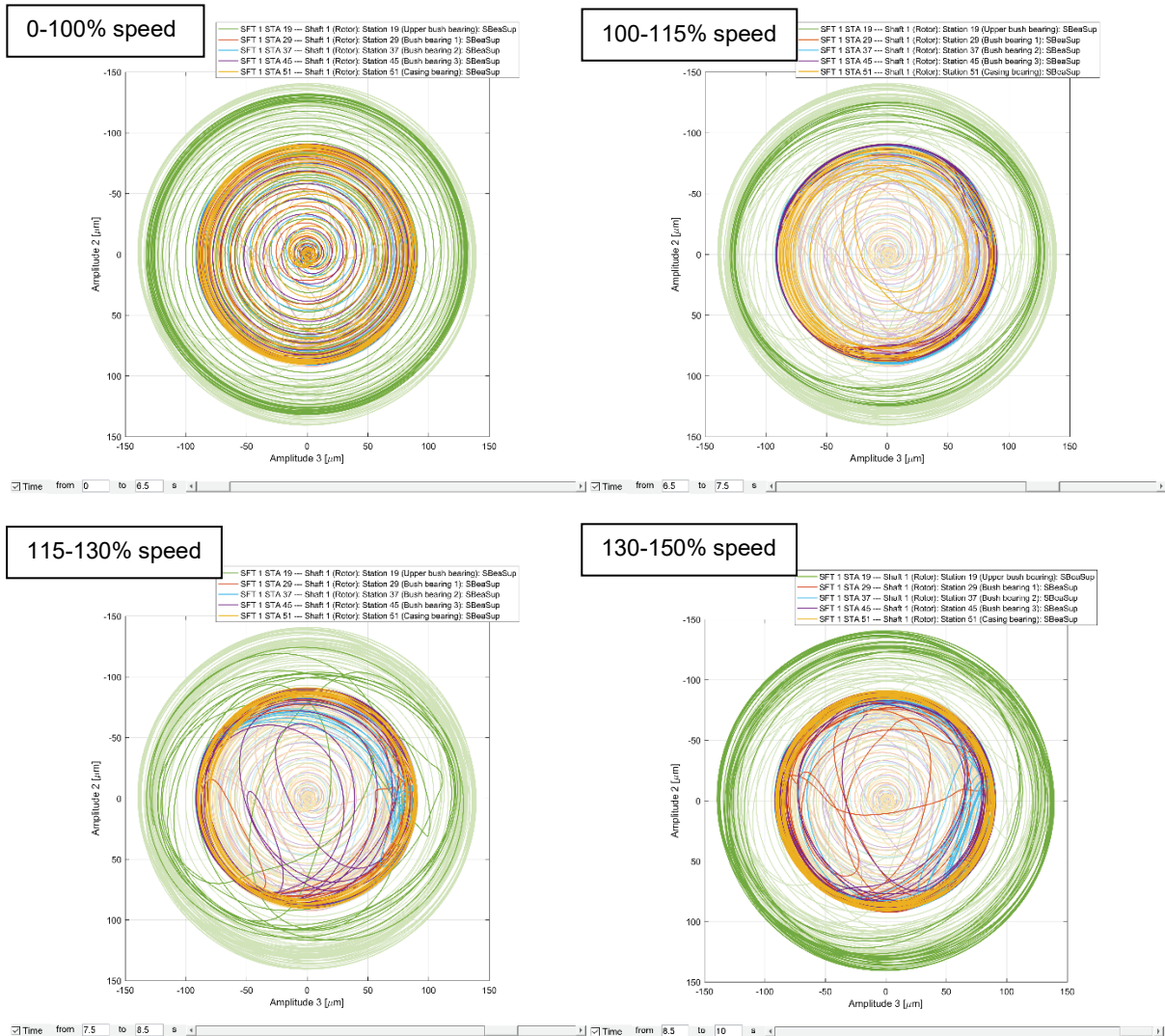


Fig. 4.3: Orbits of relative vibrations in the fluid film bearings at different speeds

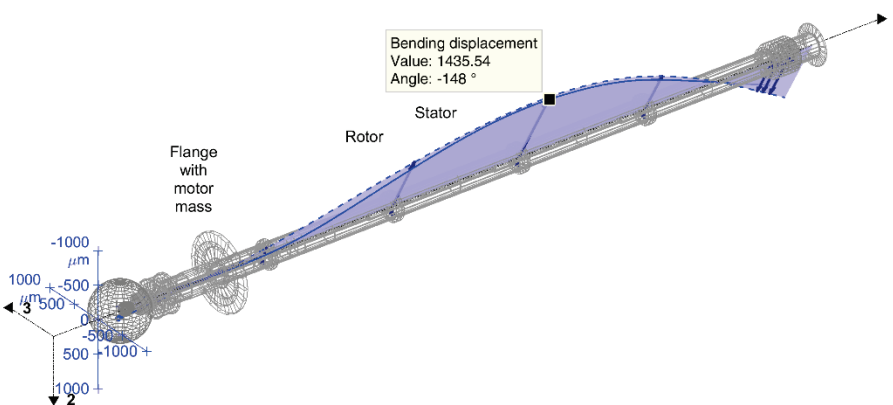


Fig. 4.4: Shape at nominal speed 1500rpm



The vibrations of the pipe indeed are huge. At 1500rpm, 100% speed the level at bush bearing 2 is about 1mm. For higher speeds it would further increase. The shape at about 1500rpm in figure 4.4 corresponds to the 2nd bending, mode 4 in figure 3.2. The dominating frequency is about 10Hz, which approximately corresponds to the frequency of this mode. The synchronous vibration caused by the unbalance is practically negligible compared to this component.

The vibration level at the ball bearing in the top is much lower than at the fluid bearings. At 1500rpm it is about 100 μ m, which corresponds to a rms value of 11mm/s. This is the location where vibrations of such machines are typically measured. Other locations with bearings are difficult to access.

The relative vibration level in the fluid bearings at nominal speed in figure 4.3 is about 90% of the bearing clearance for all bearings without considering the surface roughness, which means, that the contact stiffness just begins to become effective. At higher speeds than nominal speed rubbing phenomena can be observed due to the increasing contact force. After rubbing, which is an impact like excitation, the orbits do no longer follow the circular contour of the bearings for a short time, until they stabilize again on a circle with slightly higher radius.

Despite the high relative vibrations in the fluid bearings, the bearing forces at nominal speed are relatively low. In bush bearing 1 and 2 they are about 750N corresponding to a specific load of 1bar. The force in the rolling element bearing is about 100N, which is small compared to the axial load. This explains, why these relatively common types of machine in general work well although the vibrations at some locations are very large.

At higher speeds, where the rubbing phenomena can be observed the bearing forces are considerable higher (more than twice). At these speeds the rotor would no longer be suited for operation.

5. Conclusions

The vibration behaviour of a vertical pump supported by an angular contact ball bearing and water lubricated fluid film bearings is described. For such type of machine, a linear analysis is only suited to check the stability. Typically, such machines are unstable because of the unloaded cylindrical fluid film bearings. To determine the limit cycle of the unstable rotor, i.e. the real vibration level, a nonlinear analysis must be carried out. A load such as unbalance can be considered. In the present case a run up with an unbalance of level G10 at the pump impeller has been carried out. The dominating vibration is a sub-synchronous vibration of about 10Hz. Its amplitude increases with increasing speed. At nominal speed the synchronous vibration is negligible compared to the large sub-synchronous component. The bearing forces at nominal speed are still moderate despite the high sub-synchronous vibration level. At higher speeds than nominal speed rubbing phenomena can be observed in the relative vibrations in the fluid bearings.